THE DIGITAL MULTI-CHANNEL RADIOSPECTROGRAPH IN NANÇAY

G. DUMAS, C. CAROUBALOS*, and J.-L. BOUGERET

Laboratoire Associé au CNRS No. 264
and
Département de Recherche Spatiale, Observatoire de Paris, F-92190 Meudon

(Received 3 January; in final form 4 June, 1982)

Abstract. We describe the new Solar Radio Spectrograph which has been operated at the Nançay Radio Astronomy Station since December 1978 for the analog part (which uses photographic film data acquisition) and since July 1979 using digital magnetic recording. This instrument was designed and built by the Space Research Department of the Paris Observatory and covers the range 469–110 MHz.

The multichannel receiver yields a high sensitivity, as compared to a sweep-frequency receiver and the frequency windows where external interference is present can be eliminated from the data acquisition.

The digital recording leads to convenient intensity calibration procedures and allows a modern data-handling over a large dynamic range: 50 dB with a 11 bit resolution.

Intermodulation effects due to non linearities have been kept to a minimum by building the multiplexer as a 'tree' and distributing the amplification along.

The time resolution allows the data to be acquired at a rate of 100 samples per second per frequency channel. The frequency resolution can take two values: 120 channels 1 MHz-wide and 100 channels 200 kHz-wide can be positioned anywhere in the range 110–469 MHz.

Some observations are shown including type V and type II-like bursts and harmonically related emission in hook structures. Some future plans are briefly mentioned aiming to perform circular polarization measurements in 120 frequency channels and real time data compression.

1. Introduction

From the early days of solar radioastronomy, radio bursts have been observed with two kinds of instruments: radiospectrographs which give the intensity spectrum as a function of time (dynamic spectrum), and interferometers, linear antenna arrays and later on radio-heliographs which yield positions and sizes.

The first classification of solar bursts was mainly based upon their dynamic spectral morphology and the frequency drift rate (type I to type V bursts), whereas the moving type IV was identified from linear antenna array observations.

During the last two decades large radio-heliographs have been designed, built and operated at several discrete frequencies; they yield a wealth of new results about the association of radio bursts with coronal structures and solar activity. In the meantime many radiospectrographs have remained unchanged, still using sweep-frequency receivers and an analog output on film. This kind of instrument is certainly still very useful for the detection and identification of solar radio emission; it provides an additional information to different sets of observations related to the study of solar activity. But due to the small dynamic range and the low intensity resolution of film

* Also at Department of Physics and Electronics, University of Athens, Greece.

Solar Physics **81** (1982) 383–394. 0038–0938/82/0812–0383$01.80.
Copyright © 1982 by D. Reidel Publishing Co., Dordrecht, Holland, and Boston, U.S.A.

recording, the quality of this information is rather poor. Further quantitative analysis is severely hampered.

The spectral observation remains the basic information in solar radioastronomy, and the best way to get an outlook of a whole disturbance at various heights in the solar corona. It potentially carries in itself a lot of messages concerning the coronal magnetic field, the microstructure, and even the very mechanism of the radio emission and particle acceleration.

It is the primary way to know from the spectral feature what kind of activity or burst type, we are dealing with; apart from the well-known five burst types, the dynamic spectra have shown finer features such as pulsating structures, zebra patterns, spikes, hooks, type U and J bursts, reverse drift pairs, spike pairs, type IIIb bursts, ...

All this variety of spectral structures is now much better described using recent spectrographs of modern design. Special techniques have greatly increased the dynamic range and intensity resolution of film recording (De Groot *et al.*, 1968). And recordings which are even easier to use have been obtained by digitization (Slottje, 1974; Von Arx *et al.*, 1975, Mosier *et al.*, 1975).

But, in any case, experience has shown that, when possible, it is much more efficient to operate one's own spectrograph if it is to be used in conjunction with other instruments either on the ground or in space and if its built-in flexibility is to be fully exploited.

The instrument, which will be described here, has been designed in this context. It is a multichannel receiver covering the 110–469 MHz frequency range. Compared to a sweep-frequency receiver with the same number N of data points in the observed frequency range, the sensitivity threshold is improved by a factor $\sim\sqrt{N}$. Two sets of channels are available: one set with 120 channels and 1 MHz bandwith, one set with 20 combs of 5 adjacent channels and 200 kHz bandwidth each; they can be positioned anywhere in the observed range 110–469 MHz. In this way high resolution analysis can be performed simultaneously in different parts of the spectrum and that may serve a wide variety of research purposes.

A digital data acquisition system preserves the good sensitivity and large dynamic range of the multichannel receiver, allowing an easy calibration and a modern data-handling.

A real-time data compression system, still under test, is further described; it would retain the high time resolution only when it is needed, saving storage support and increasing the observing time, the number of recorded frequency channels and/or the sampling rate. A further development of the instrument to make circular polarization measurements in 120 channels is also scheduled.

The frequency range 469–110 MHz was chosen because it corresponds to coronal layers extending from the top of the chromosphere to about $0.5 R_{\odot}$, that is near the transition altitude between closed and open solar magnetic structures.

The instrument, designed and built by the Space Research Department of the Paris Observatory, is also used to support space experiments such as the radio experiment on board ISEE 3, and other observing facilities at the Nançay station, especially the radio-heliograph and the decametric array.

Design considerations of the spectrograph and main technical solutions retained are described in an engineering journal (Dumas, 1982).

2. The Multichannel Spectrograph

The instrument consists of a wide band antenna, a multichannel receiver and a data acquisition system.

2.1. The antenna

The antenna is made of a 6-meter dish on a equatorial mount. The design of a wide-band focal system to measure circular polarisation has always been a difficult problem (Van Nieuwkoop, 1971; Dumas, 1978a, b). The main difficulty is to design and build an antenna as well matched to its transmission line as possible over a large bandwith while retaining a high-signal rejection between the two linearly polarized channels. Imperfections in the impedance matching result in large variations of the sensitivity as a function of the frequency. The focal system of the Nançay equipment is made of two crossed log-periodic antennas. The rejection obtained between polarities varies from 26 dB (at 126 MHz) to 36 dB (at 460 MHz). It is an adaptation of the one used in Dwingeloo (De Groot and Van Nieuwkoop, 1968; Van Nieuwkoop, 1971). At the present time, observations use one linearly polarized antenna, and the sensitivity variation over the whole frequency range is less than 3 dB. The preamplifier is temperature compensated and its gain variations are extremely small. The measurement of polarization will be obtained by combining the two linearly polarized antenna signals through a 90° hybrid circuit.

2.2. The receiver

A drawback of multichannel receivers as compared to sweep frequency receiving system, is their much larger hardware complexity. Indeed, each independent channel requires at least a mixer stage followed by an intermediate frequency (IF) amplifier with the proper input/output (I/O) response.

One is also faced with two main design problems:

– The increased risk of intermodulation due to the large overall bandwith.

– The spurious effects resulting from the use of numerous local oscillators (LO), the frequency harmonics of which can beat together to produce a lot of undesired cross products and as many signal spurious responses.

The first problem is solved in the filter bank by distributing the amplification among the different stages of the 'tree' of power and band splitters, i.e. by avoiding high gains over widebandwiths. Interference from LO harmonics is controlled by a careful design of the 'matrix of mixers' and a thouroughly planned distribution of the LO frequencies.

2.2.1. *The filter bank* including power splitters, associated with appropriate filters, makes a 'tree' (Figure 1) which divides successively by two the power as well as the frequency bandwidth. The resulting power losses are balanced by means of amplification distributed at each dividing step; so that, the risk of intermodulation is kept to a

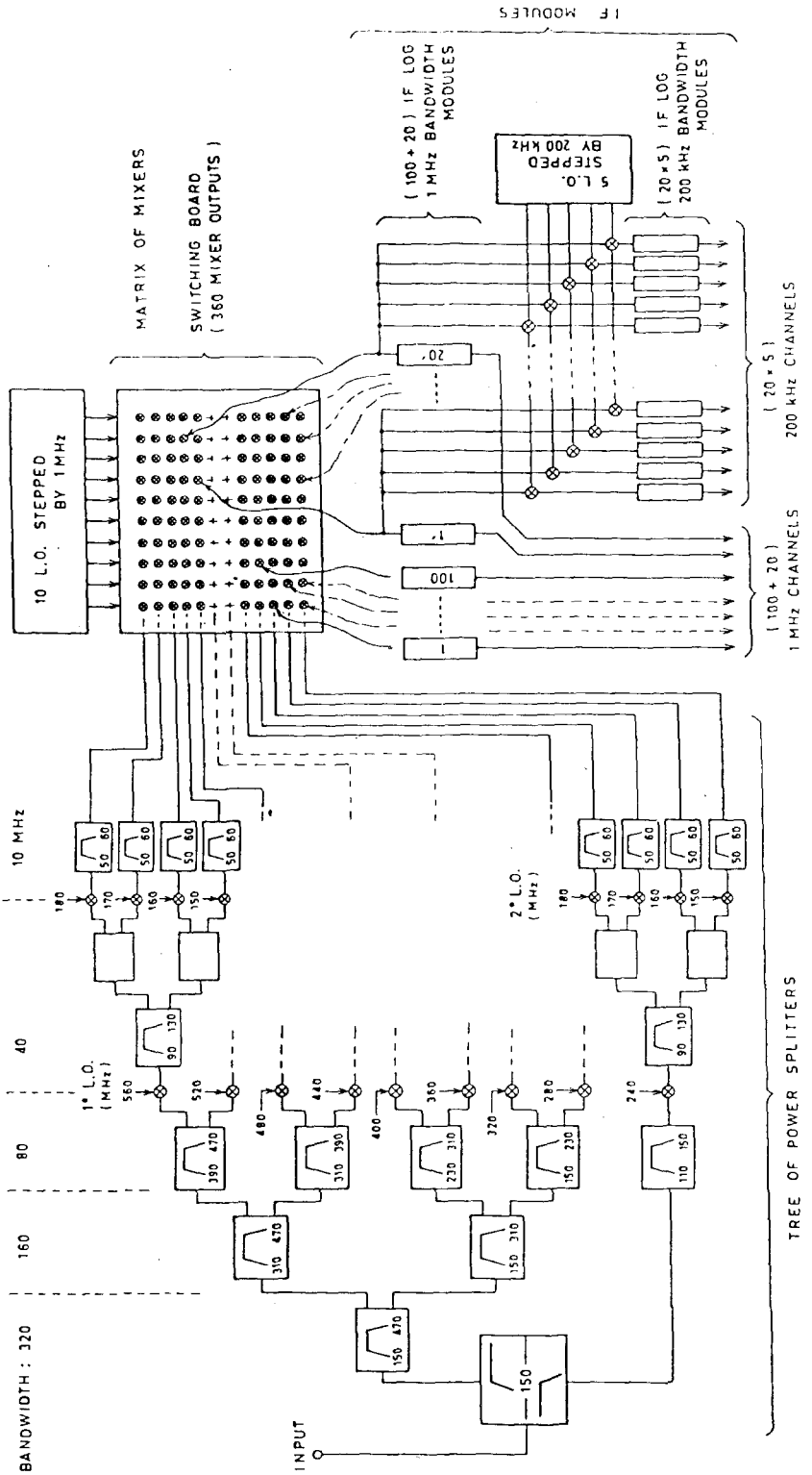

Fig. 1. Spectrograph receiver block diagram.

minimum. Moreover, such an active multiplexer avoids most of the difficulties which occur with paralleling filters. Two main steps of mixing are involved: the input signal is distributed into nine 40 MHz-wide channels centered on the same frequency (110 MHz). Then each of these frequency bands are split again into four 10 MHz-wide channels, all centered on 55 MHz. Thirty six 10 MHz-wide channels are then obtained, each of them feeding a line of the 36 × 10 matrix of mixers. This arrangement is complemented by a rejection filter against the local TV transmitter frequency. So that we have never been able to see any effects of the residual non linearities in the I/O response even in the presence of strong interferences.

2.2.2. The 10 columns of the matrix of mixers are fed by 10 local oscillators, the frequency of which differs by 1 MHz from each other. So that each elementary mixer of the matrix produces a frequency shift of its input signal, 10 MHz-wide, in order to finally center all parts of the overall frequency window on the same frequency of 15 MHz. In that way all IF amplifiers can be made identical. The design of the matrix of mixers allows the selection of any frequency in the range 110–469 MHz by steps of 1 MHz (360 positions).

2.2.3. *The IF modules* (see Figure 2) determine the final IF pass band of the channel (1 MHz or 200 kHz), the I/O response and finally set the overall transfer function of the system: logarithmic response over a dynamic range of 50 dB.

Let us summarize the advantages of the logarithmic response: gain stability in the IF channels and increase of the dynamic range without gain switching. Moreover it is known that the relative RMS fluctuation of the detected noise output I ($\Delta I/I$) is constant, that is independent from I. So that the linear A/D conversion of a logarithmic output will keep the digitization error matched to ΔI.

The number of independent data outputs is limited by the number of complete IF modules which can be reasonably built and maintained. We use 120 (1 MHz) modules and 100 (200 kHz) modules. In routine configuration we are presently recording 115 channels on film and 32 on tape. The 115 channel frequencies are logarithmically spaced

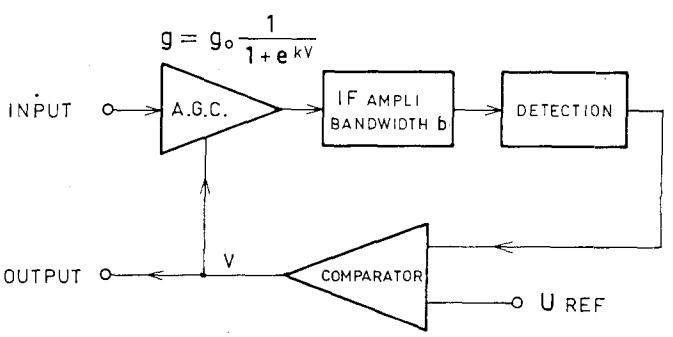

Fig. 2. IF module block diagram.

over the 110–469 MHz range, so that each frequency is 1.012 times its lower neighbouring one ($\Delta f/f = 1.2\%$).

This distribution is well adapted to the study of solar radio phenomena which show a nearly constant relative spectral bandwidth $\delta f/f$; such are the type III bursts and fundamental-harmonic phenomena.

2.3. The calibration system

The intensity calibration of the radio receiver is triggered either automatically or upon request. It consists of two steps:

– In the first calibration step, a matched solid state noise generator is switched into the system and replaces the antenna. Its noise temperature is 10 600 K and it may be considered as a reference level.

– In the second step the logarithmic response of the system is measured using a much higher noise level which is progressively reduced by steps of 1 dB over a range of 64 dB.

However the overall system calibration (including antenna gain calibration) is to be performed by observing known radio sources (for instance Cygnus A) at discrete frequencies where the antenna matching is best.

3. The Data Acquisition System

The information is recorded in both analog (35 mm film) and digital form (800 BPI tapes). The two systems are totally independent. The maximum number of channels which can be digitized with our current data acquisition system cannot exceed 64. On the contrary all the 115 channels are displayed on film during routine observations in the entire frequency domain. This is very useful to some studies when only qualitative high sensitivity spectral information is needed.

3.1. The display of the dynamic spectrum on film

The output voltage of the 115 IF modules (either 1 MHz or 200 kHz bandwidth) are separately connected to a row of 115 light emitting diodes (LED) through 115 interfaces. The intensity response of the interfaces is chosen to preserve the logarithmic response of the receiver and so to favour the intensity resolution at low and intermediate signal levels. The overall on-film dynamic range is increased by the fact that the size of the LED light source increases with its brightness. Time is decoded from the Swiss PRANGINS transmitter (HBG) and appears as dots every second and in clear every minute. The current film speed is 0.250 mm s^{-1} which provides a resolution of ≈ 0.1 s.

3.2. The digital data

In the present configuration without data compression only 32 output voltages among the 220 IF outputs are sent to 32 active filters whose cut-off is matched to sampling rates selected in the set 1, 2, 5, 10, 20, 50, 100 Hz. The spectral information is extended by the acquisition of three frequencies of the LF domain (75, 60, 30 MHz) obtained from separate radiometers of the Nançay station. In the data acquisition system are also

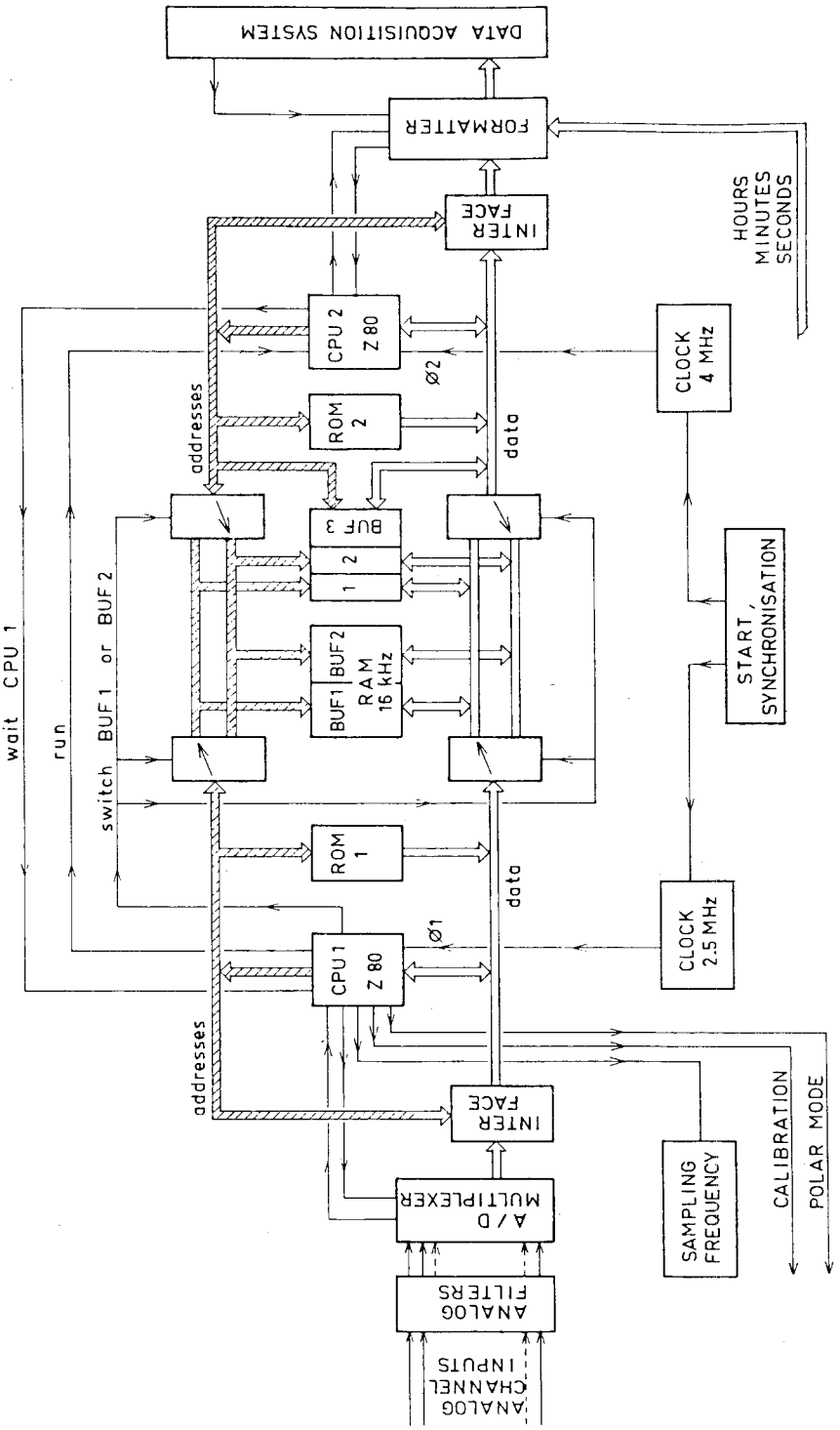

Fig. 3. Data compression system block diagram.

recorded six other channels from a 3-antenna multicorrelator interferometer which yields the 2-dimensional position of radio bursts at 75.5 MHz (Daigne *et al.*, 1975). The resulting 42 output voltages are multiplexed and converted into 11-bit words providing an accuracy of ≈ 0.02 dB for an intensity range of 50 dB. Routine observations of the Sun are currently made at the rate of 10 Hz, yielding 6 hours of observation per magnetic tape. Further data processing is made on computers: the SOLAR 16/65 of the Space Research Department and the Observatory VAX 11 in Meudon.

3.3. Data compression

A more elaborate digital data handling system has already been tested by simulation, and its realization is in progress. It will allow observation of both senses of circular polarization. It handles 12 800 2-bytes words by second. Two Z-80 microprocessors are used. The first of them controls the input-output command along the buslines and handles the on-line software programs. The second performs the necessary digital computations. The overall operation is seen in Figure 3.

120 output voltages of 120 selected IF modules are filtered, multiplexed and digitized at the rate of 100 Hz. Let us first see the data compression algorithm for one channel (Rosso, 1979). The digital signal is divided into successive 'sentences' of a given constant number N of data point $x_{i,j}$ where i and j denote the current timing indices of the data points and of the sentence respectively. Let m_j be the arithmetic average of the N data points in the sentence j. If the quantity $\mu = \sum_i |x_{i,j} - m_{j-1}|$ computed in the jth sentence is smaller than a given limit σ, then the sentence is deleted and only the average m_j is kept and recorded together, with the time. If μ is greater than σ, all the data points in the sentence are transmitted. So a very detailed description of the signal is performed only during active periods. By properly choosing N and σ, this algorithm seems to nicely describe even the weak bursts.

In practice, the signal processing which leads to the decision of keeping or not sentences is performed on only three 'master-channels'. If the decision is positive, then the data from all other channels is also kept. During routine observations, the master-channel frequencies will be set at 169 MHz (the Nançay radioheliograph observing frequency) and at two other frequencies in the upper and the lower frequency observing range. The values of the parameters of the compression algorithm result from a trade-off between the compression efficiency (ratio of the total number of data points acquired to the number of the retained ones) and the acceptable level of degradation of the signal. We are anticipating an average compression ratio of 20 to 80 for the highest time rate. We are planning to subdivide the overall received frequency range into sub-bands, each of them being monitored by a master-channel.

4. Early Results

We give below some examples of early observational results both on film and digital form. All of them are obtained in routine configuration (1 MHz bandwidth with logarithmic distribution).

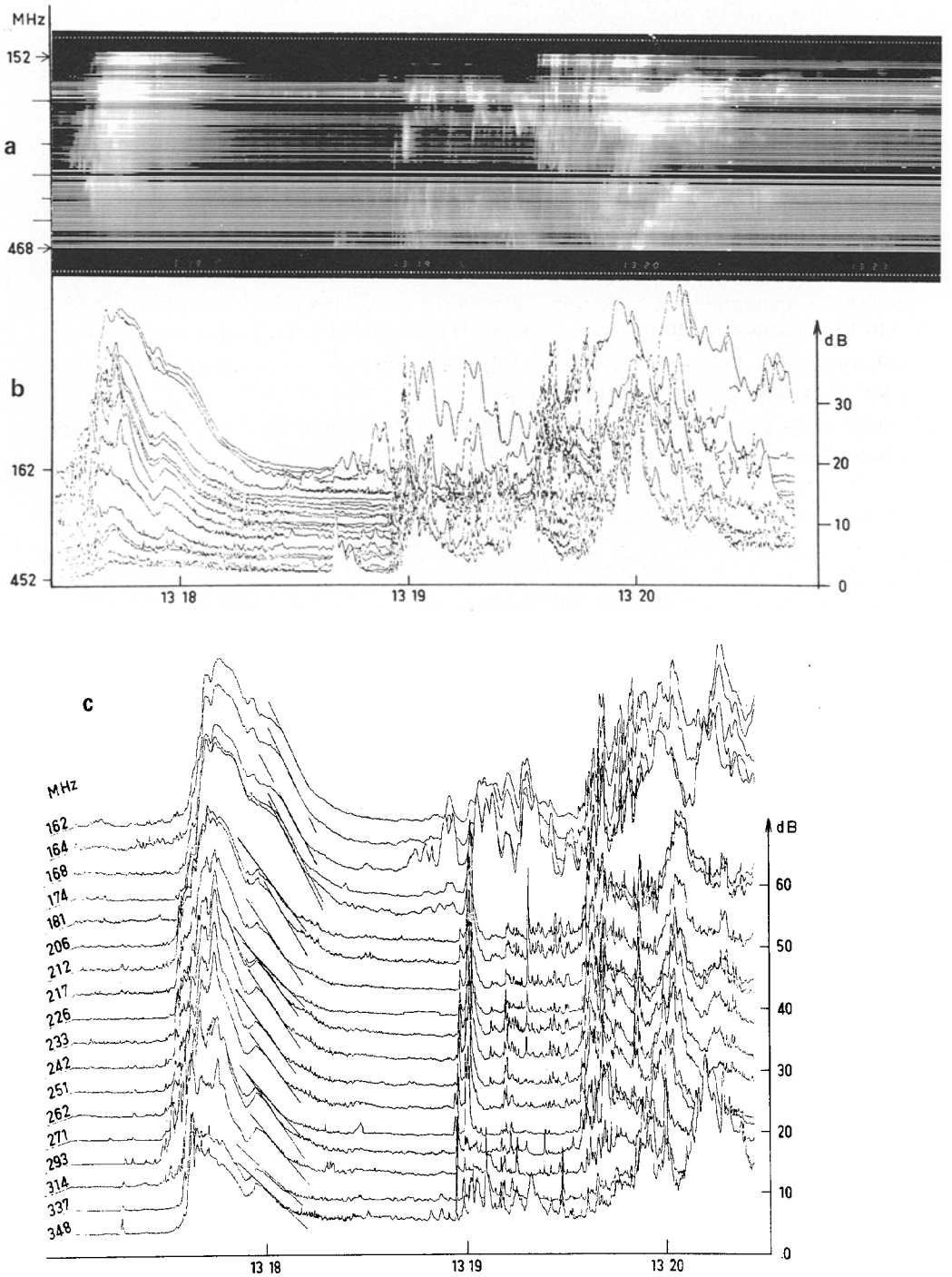

Fig. 4. The complex radio event of May 7, 1980 (a) 100 channels in film output, (b) and (c) the channel digitized outputs.

4.1. THE EVENT OF MAY 7, 1980

This event presents a couple of exceptional features that we briefly describe in the following. The film display provides a detailed view of the event in the band 152–468 MHz (Figure 4a).

A first group of activity starting at about 13:17:30 UT, shows a rise-front with a general drift rate typical for type III bursts, but with no definite continuity in the frequency domain suggesting a complex coronal region. The end of this first group is typical of a type V burst. The real nature of type V emission is still being discussed, and some observers argue that they are just the superposition of a large number of type III's giving the appearance of continuity. This is the case where the film display alone is definitely inadequate to remove the doubt. The digitized time profiles (Figures 4b, c) show very smooth profiles even on the high frequency side, which is hard to obtain just with a superposition of individual bursts.

Our data provide another argument: Figure 5 shows that the decay time τ for this event increases with frequency.

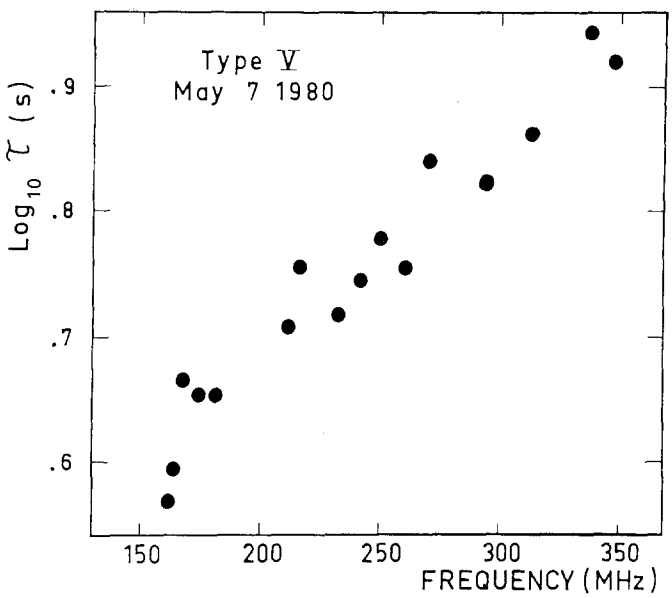

Fig. 5. Decay time τ versus frequency for the type V of May 7, 1980, 13:18 UT event, measured on Figure 4c.

These results are utterly different from both the usual values and the frequency dependence of the decay time for type III bursts, which would have been expected in the case of a superposition of type III's. This point is certainly of high importance in the understanding of type V mechanisms and will require further investigation.

The second group of activity starts around 13:18:55 UT and lasts about 1.7 min in the 152–468 MHz band. It provides dramatic evidence for fundamental-harmonic (FH)

emission, and in the present paper we will restrain the discussion to this evidence. A series of at least 3 FH 'hooks' are well identified. The advantage of the logarithmic distribution of the frequencies in the band under observation on that day (468–152 MHz) clearly shows here: the FH hooks have about the same shape since the ratio $\Delta f/f$ is kept about constant. Such bursts christened 'hooks' by Ellis (1969) and also studied by Møller-Pedersen (1978) are usually observed in the decameter wavelength range and have never been reported in the metric range. At variance with these previous observations, our 'hooks' have not the multiple traces, characteristic of drift pairs. Yet they are clearly not coincidental crossings of forward and reverse drift type III's, and the second component is more diffuse than the first, just as in the decametric observations. Moreover, FH emission has never been mentioned and the current theories do not predict it. The peculiar shape of the burst enables us to measure the harmonic ratio with some accuracy: the top of the sharp bend between the two opposite frequency drifts is taken as reference. Though its physical meaning is unclear, this sharp bend allows a very accurate determination of the two component frequency ratio which cannot be obtained for similar studies in FH structures of type III or even type U bursts. For the three FH hook pairs, the harmonic ratio is respectively: (1) (378 ± 3) MHz/(187 ± 2) MHz $= 2.02 \pm 0.04$; (2) (402 ± 11) MHz/(206 ± 2) MHz $= 1.95 \pm 0.08$; (3) (431.5 ± 5) MHz/(215 ± 2) MHz $= 2.007 \pm 0.04$. The three pairs together yield a FH ratio 2.006 ± 0.026.

Another important parameter to discuss the FH phenomena is the eventual existence of a time delay between both harmonic features (Stewart, 1976). Indeed if the fundamental is emitted close to the plasma frequency, the refractive index is close to zero and a group delay is expected. It can be estimated by comparing the timing of the fundamental to that of the harmonic which should not undergo such a group delay. Again the peculiarity of the hooks makes possible a more accurate measurement from the digital intensity-time plots. Two FH hook pairs can be measured without ambiguity. The pair at 13:19:04 UT yields a delay $t_F - t_H = 0.6 \pm 0.15$ s. The pair at 13:19:26 UT yields $t_F - t_H = 0.4 \pm 0.25$ s. The relatively poor accuracy is due to the limited number of channels rather than to the time resolution (20 points s^{-1}). Both measurements together yield a delay of 0.5 ± 0.2 s. A simple approximation (see for instance Wild *et al.*, 1959) shows that $\Delta t = (\text{Log } 2 - \text{Log } (1 + \sqrt{1 - (f_p/f^2)}) \times 2H/c$ (f_p local plasma frequency; H = density scale height; c velocity of light). The observed delay requires that the fundamental is generated (i) close to the plasma level and (ii) in region where the density scale height is not too small.

The last part of this event also shows interesting features: slow drift FH emission made of very rapid drift structures, denoting an emission with $\delta f/f \simeq 0.25$ at discrete times, without the usual continuity observed during type III's or type II's. The drift velocity is too small for an usual type III, and too large for a type II. The original film display better shows that the drift culminates and starts to reverse at about 13:20:12 UT, hinting at a type U like or an 'inverted J' type, the slow drift being related to a higher density scale height probably due to the presence of a coronal condensation with a smaller density gradient.

Acknowledgements

Historically, solar multi-channel spectrography in the metric wavelength range has been provided at the Nançay Radio Astronomy Station by the Space Research Department of the Paris Observatory, mainly for the purpose of basic spectral identification during current solar burst space experiments. It started in 1971 with a simple 16-channels spectrograph. Then one of us (C.C.) obtained support from CNRS to start the present project which later became full part of the program of the Laboratoire Associé au CNRS No. 264 (LA 264). The project was also sponsored by the INAG and the Paris Observatory.

We thank the Director of the LA, J. L. Steinberg, and G. Epstein for valuable help, the second one suggesting the basic ideas of the sentence compression. We also thank all the engineers and technicians of this Laboratory who participated in the project; namely M. Rosso, who studied and designed most of the digital handling system; R. Bru, D. Carrière, Y. Guillou, R. Hulin, G. Huntzinger, M. Liepschitz, J. P. Mengué, V. D. Phan, and A. Rapin. We particularly thank B. Clavelier and C. Rosolen for their assistance. We are grateful to J. Van Nieuwkoop for providing details on the antenna he designed for the Dwingeloo spectrograph. Thanks also go to the Nançay Radio Astronomy station for welcoming the project and providing the antenna reflector and mount. We are particulary grateful to J. Renaud who currently runs the observing program, C. Chantelat and A. Gerbault who help this program. Digital data are processed on the SOLAR-16/65 of the Space Research Department and the VAX 11 of Meudon Observatory. Finally Mrs R. Crepel and MM. C. Perche and G. Goyon are thanked for their essential contribution to the film reduction and digital data processing.

References

De Groot, T. and Van Nieuwkoop, J.: 1968, *Solar Phys.* **4**, 332.
Daigne, G., Caroubalos, C., and Poquérusse, M.: 1975, Report 131/DESPA Meudon Observatory.
Dumas, G.: 1978a, Report 172/DESPA, Meudon Observatory.
Dumas, G.: 1979b, Report 179/DESPA, Meudon Observatory.
Dumas, G.: 1982, *l'Onde Electrique*, submitted.
Ellis, G. R. A.: 1969, *Australian J. Phys.* **22**, 177.
Kane, S. R. and Raoult, A.: 1981, *Astrophys. J.*, in press.
Møller-Pedersen, B.: 1978, Thesis, Univ. Paris VII.
Mosier, S. and Fainberg, J.: 1975, *Solar Phys.* **40**, 501.
Rosso, M.: 1979, Doctoral Thesis in Engineering, CNAM, Paris.
Stewart, R. T.: 1976, *Solar Phys.* **50**, 437.
Slottje, C.: 1974, *Astron. Astrophys.* **32**, 107.
Van Nieuwkoop, J.: 1971, Thesis, Univ. Utrecht.
Von Arx, B., Benz, A., and Tarnstrom, G.: 1975, *Bull. Am. Astron. Soc.* **7**, 407.
Wild, J. P. and Smerd, S. F.: 1972, *Ann. Rev. Astron. Astrophys.* **10**, 159.
Wild, J. P., Sheridan, K. V., and Neylan, A. A.: 1959, *Australian J. Phys.* **12**, 369.